International Journal of Numerical Modelling: Electronic Networks, Devices and Fields

WILEY

RESEARCH ARTICLE

Spoof Surface Plasmon Polariton Enables Ultrawideband THz Absorption Enhancement of Multilayer Graphene Excited by a Double Circular Metal Ring Array

H. E. Guo-Qiang[1] | Tingyue Sun[2] | Zhen-Yu Ding[2] | Siqi Xu[2] | Cheng Chen[3,4] | Cathleen De Tandt[3] | Muhammad Muneeb[5] | Dries Van Thourhout[5] | Bart Kuyken[5,6] | Johan Stiens[3,7]

[1]Key Laboratory of Specialty Fiber Optics and Optical Access Networks, Joint International Research Laboratory of Specialty Fiber Optics and Advanced Communication, Shanghai University, Shanghai, People's Republic of China | [2]School of Communication and Information Engineering, Shanghai University, Shanghai, People's Republic of China | [3]Department of Electronics and Informatics ETRO-IR of the Faculty of Engineering, Vrije Universiteit Brussel (VUB), Brussels, Belgium | [4]School of Information Science and Technology, Northwest University, Xi'an, People's Republic of China | [5]Photonics Research Group, Ghent University, Gent, Belgium | [6]Center for Nano and Biophotonics (NB-Photonics), Ghent University-IMEC, Ghent, Belgium | [7]SSET Department, IMEC, Leuven, Belgium

Correspondence: Siqi Xu (siqixu0825@163.com)

Received: 13 March 2026 | **Revised:** 9 June 2026 | **Accepted:** 16 June 2026

Keywords: absorber | double circular metal ring (DCMR) array | graphene | spoof surface plasmons polaritons (SPPs) | terahertz (THz)

ABSTRACT

Although graphene's THz absorption rate increases with number of graphene layers, the absorbance is limited and unsatisfactory as a practicable absorber. Patterned graphene or graphene-based surface plasmon resonance has been proved to enhance THz absorption, but the performance is prone to be affected by graphene defects and local multilayer stacks. In this paper, we proposed to use a double circular metal ring (DCMR) array to enhance both the graphene's THz absorption with an ultrawide bandwidth and the tolerance of graphene's physical impurities. A DCMR array is patterned on the top surface of graphene layer with dielectric substrates, which excites a broadband spoof surface plasmons polaritons (SPPs) in the THz frequency range. The broadband spoof SPPs locally confine and strengthen THz wave interaction with graphene, and further enhance graphene's THz absorption, which is confirmed by numerically simulated dispersion relations. A four-layer graphene composite structure is fabricated to validate the scenario, which consists of graphene, a SiO_2-capped doped-silicon substrate covered by graphene, and the DCMR array on the top surface of graphene. Time domain spectroscopy test shows that the THz absorption enhancement of the graphene composite with DCMR array covers the frequency range from 0.3 to 1.1 THz with 110% bandwidth. The THz absorption of the proposed graphene composite increases to more than 70% over a wide bandwidth of 77% at 0.65 THz compared with the graphene composite without DCMR array.

1 | Introduction

Various terahertz (THz) applications, including imaging, sensing, and wireless communication, require high-end THz building blocks. THz absorber is one of the key components of these applications. Therefore, the search for materials and design solutions with broadband and high-absorption properties is becoming a research focus. The traditional terahertz absorber typically employs a three-layer structure consisting of a metallic resonator layer, a dielectric spacer layer, and a metallic reflector layer, achieving high absorptivity by capturing terahertz waves with the patterned top metal and realizing zero transmission with the continuous bottom metal [1, 2]. To realize tunability, an additional tuning layer is introduced [3]. This tuning layer is usually made of surface plasmons polariton (SPP) materials, including noble metals (e.g., gold, silver) and two-dimensional

[Correction added on 14 July 2026, after first online publication: The Special Issue linked has been removed in this version.]

materials (e.g., graphene), where the former exhibit strong field confinement and low loss in the visible to near-infrared range, while the latter support highly tunable plasmons in the terahertz and mid-infrared ranges. Among these, graphene's wideband electromagnetic behavior makes it a promising nanomaterial for THz absorbers. However, despite extensive research into the electromagnetic properties of graphene, its intrinsic terahertz absorption remains very limited [4–7]. Many researchers aim to improve graphene's THz absorption. In general, two different routes have been investigated to enhance the absorption.

The first approach involves patterning graphene on a layered dielectric substrate to create graphene metamaterials. Such method uses the resonant effects of the metamaterials along the graphene normal direction to enhance terahertz absorption. Studies have reported various patterned graphene structures with different geometries, achieving dual-band, multiband, and even ultrabroadband terahertz optical absorption enhancement [8–14]. For example, patterning single-layer doped graphene into periodic nanodisk arrays enables 100% optical absorption at the resonance frequency [15]. Similarly, metamaterials based on sinusoidally patterned graphene can achieve impedance matching with incident waves in free space, leading to broadband and exceptionally high terahertz absorption [16]. The absorption performance of the graphene metamaterials with patterned graphene above largely relies on graphene's quality. By electronically doping graphene, graphene metamaterials show tunable light absorption property and reconfigurable frequency [17–19]. However, an extremely high bias voltage has to be exerted on the graphene to achieve high THz absorption ability, which modulates its chemical potential to a high level. A 90-nm-thick graphene metamaterial absorber is reported with approximately 85% absorptivity of unpolarized light across the visible and near-infrared spectra, covering the entire spectrum from 300 to 2500 nm [20]. The downside is that this broadband, high-absorption performance requires a complex fabrication process involving multiple layers of graphene and a dielectric substrate.

The second approach utilizes graphene surface plasmons resonances to locally trap THz light, enhancing the interaction between THz waves and graphene and thereby increasing THz absorption [21–29]. Graphene cut-wire arrays are used to realize tunable metasurfaces responding in the terahertz regime. By optimizing the geometry of graphene cut-wire, a maximum 50% absorption can be achieved [23]. Gali et al. designed a broadband tunable terahertz absorber by constructing a subwavelength grating from a single-layer graphene metasurface with one-dimensional periodic doping. This design achieves the theoretical absorption limit and an ultrawide bandwidth of up to 185%, demonstrating strong light–matter interaction at subwavelength scales [28]. By reshaping the flat graphene into complex three-dimensional (3D) pillars, Song et al. observed strong high-order plasmonic modes verified by numerical calculations and experimental results [29].

The graphene designs mentioned above require high-quality monolayer graphene, which is hard to obtain in practice. State-of-the-art fabrication methods, such as chemical vapor deposition (CVD), produce graphene samples with local defects and multilayer overlaps. These imperfections severely degrade graphene-based THz absorbers, especially those with patterned graphene structures. A 3D graphene foam prepared through the solvothermal method shows 95% bandwidth with 90% THz absorption, and is also able to tolerate local defects. However, the thickness of the graphene foam reaches 4 mm, which is very thick compared with other graphene absorbers [30]. We previously used a double circular metal ring (DCMR) array patterned on a monolayer graphene to enhance modulation depth of graphene-based THz modulators [31]. With further investigation, we observed that the scenario of the DCMR array on graphene design can mitigate the defects and overlaps of graphene samples while achieving high THz absorption ability with ultrawide bandwidth. In this paper, we discuss the physical mechanism behind this THz absorption enhancement and experimentally validate the concept.

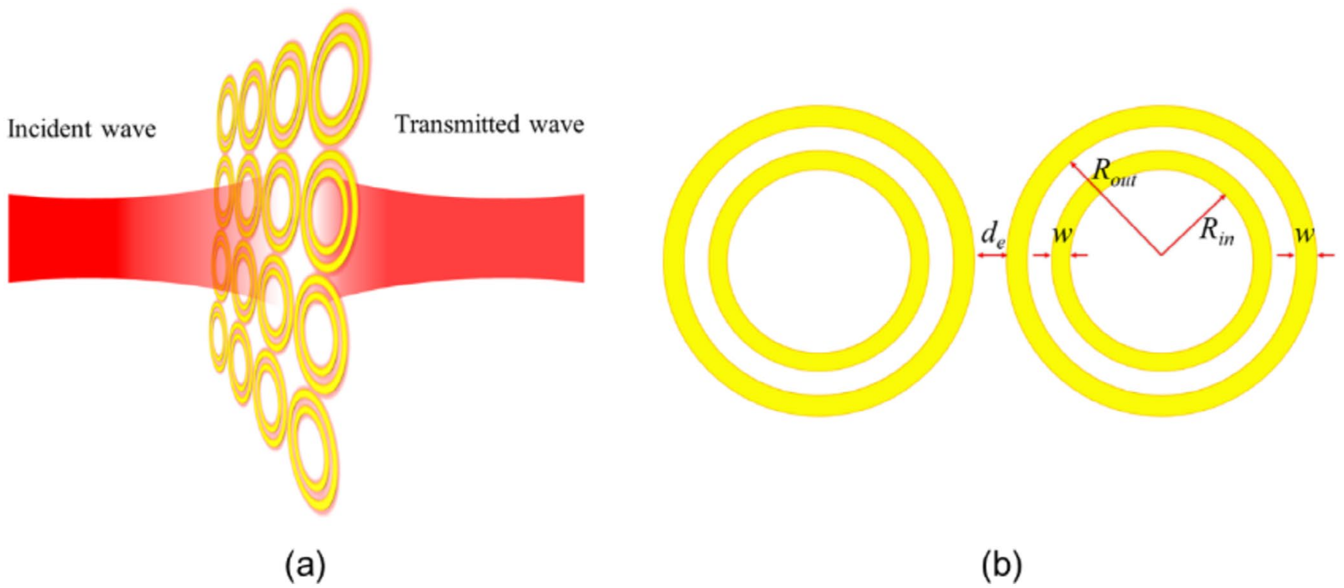

FIGURE 1 | Schematic diagram of THz light interaction with the DCMR array: (a) 3D view of the schematic diagram; (b) top view of two adjacent DCMR units.

2 | Methods and Experiments

Figure 1 shows the schematic diagram of THz light interaction with the DCMR array. The geometrical parameters of the DCMR shown in Figure 1b are chosen as $R_{in} = 34\,\mu m$, $R_{out} = 44\,\mu m$, $w = 2\,\mu m$, and $d_e = 4\,\mu m$. The details of structure optimization process are discussed in Supporting Information.

The dispersion relation of the DCMR has been numerically calculated by employing the eigenmode solver of commercial software CST Microwave Studio, and is presented in Figure 2. It shows that the DCMR excites the spoof SPPs. The slow wave behavior of the DCMR SPPs is activated at $d/\lambda = 0.247$. A broadband dispersion property is observed in the whole Brillouin zone form X to M, reaching the maximum at M, and disappears in the middle period of M to Γ.

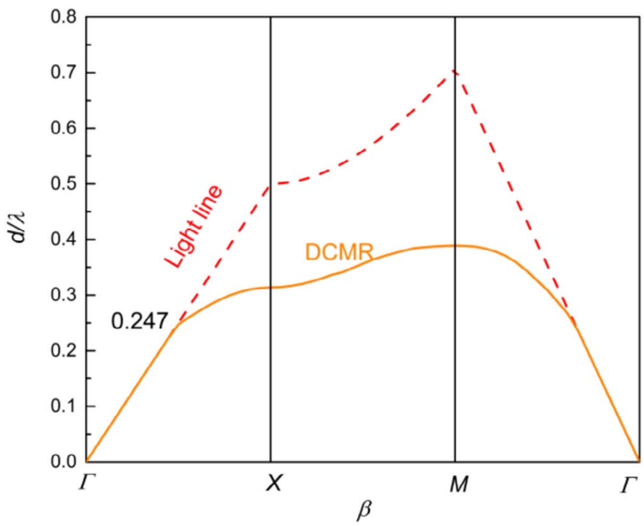

FIGURE 2 | Dispersion diagram normalized to the unit cell dimension d of the DCMR.

To prove the broadband SPP properties of the DCMR, the intensity of electric field z-axis component distribution on the DCMR array is presented in Figure 3 at different frequencies from 0.30 THz to 1.10 THz for the chosen DCMR size. The incident THz wave impinging on the DCMR array excites the spoof SPPs. The electric field intensity increases with frequency from 0.30 to 0.90 THz and reaches the maximum at 0.90 THz. When the frequency rises over 0.90 THz, the electric field intensity gradually weakens, and can be observed at 1.10 THz as is shown in Figure 3i. It illustrates that the DCMR loses the confinement of the SPPs' surface waves. The broadband DCMR SPPs confine the incident THz waves on its surface of the DCMR array. The local THz wave confinement of the DCMR SPPs shows the potential of enhancing interaction between graphene and THz wave, thus further increasing graphene's THz absorption ability by depositing the DCMR array on the top surface of graphene.

Two multilayer graphene samples bought from Graphenea Company are chosen for the experiments. The graphene samples are substrated by SiO_2 and highly doped silicon layers, which forms a graphene composite. One of the graphene samples is patterned with DCMR array by using the evaporator deposition technique with designed pattern masks as is illustrated in Figure S3. In order to guarantee accurate alignment between the masks and graphene samples, boundary marker is added on the four corners of the masks. Gold is chosen as the metallic material of the DCMR array on the graphene composite attributing to the excellent conductivity and easy to pattern on the graphene. The minimum metallization pattern size is below $0.5\,\mu m$, which makes the DCMR array with the minimum size $2\,\mu m$ as shown in Figure 1 realizable. The thicknesses of the SiO_2 and silicon layers are 300 nm and 500 μm,

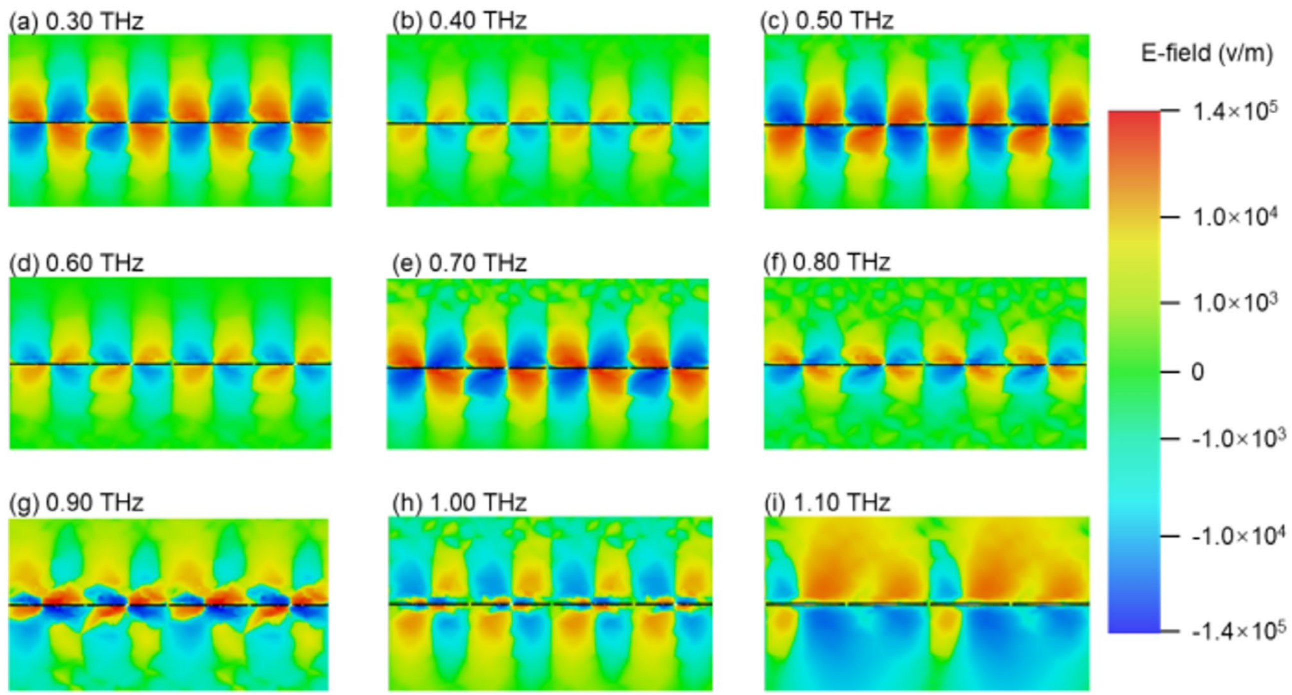

FIGURE 3 | Electric field z-axis component distribution of the DCMR SPPs on the DCMR array versus frequency: (a) 0.30 THz; (b) 0.40 THz; (c) 0.50 THz; (d) 0.60 THz; (e) 0.70 THz; (f) 0.80 THz; (g) 0.90 THz; (h) 1.00 THz; (i) 1.10 THz.

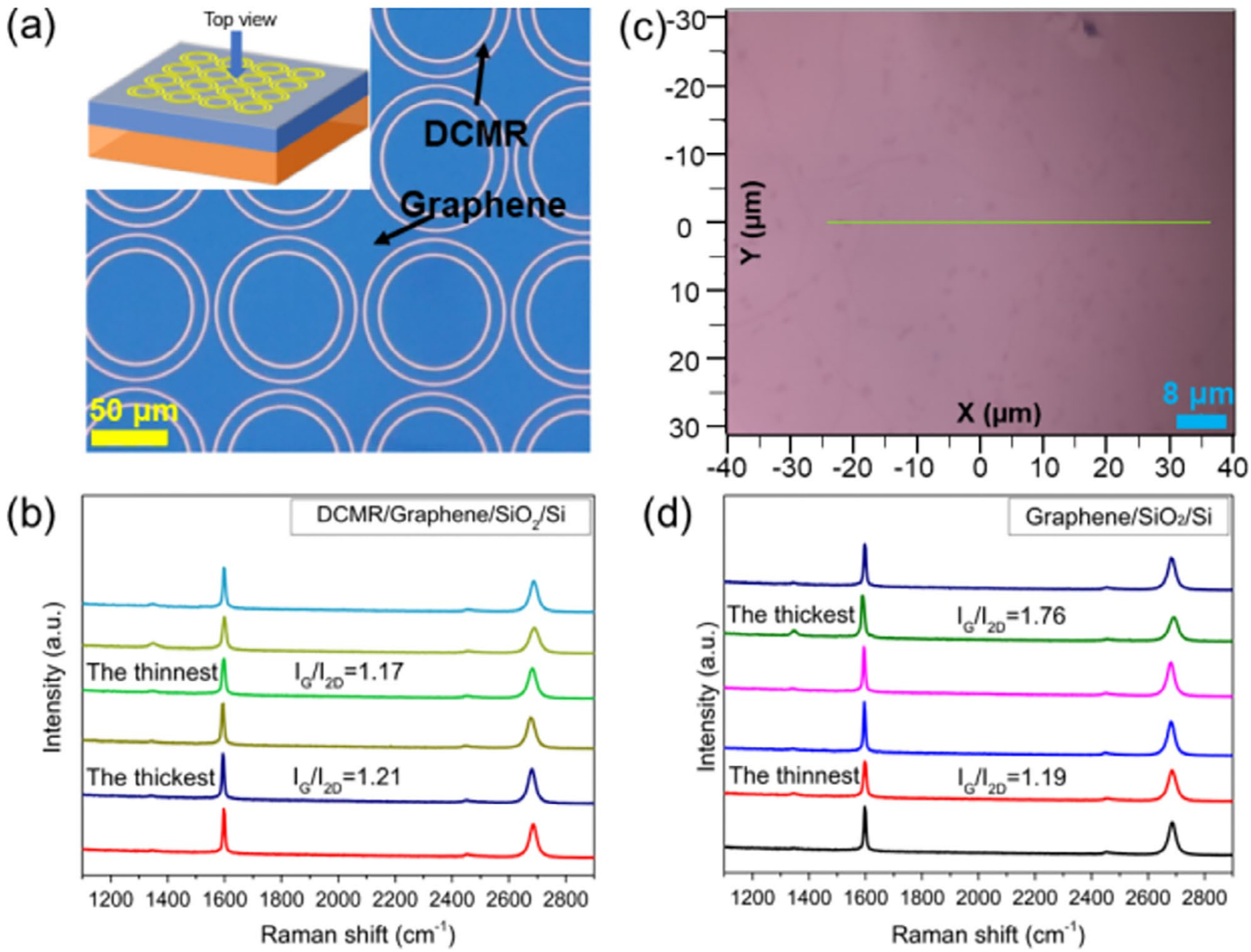

FIGURE 4 | (a) Top view of graphene composite with DCMR array, inset: Schematic diagram of graphene with DCMR; (b) Raman spectroscopy of graphene composite with DCMR array; (c) Top view of graphene/SiO_2/Si sample; (d) Raman spectroscopy of graphene/SiO_2/Si samples.

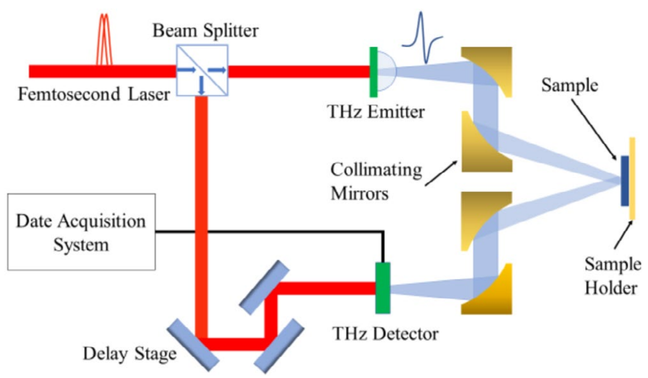

FIGURE 5 | Schematic diagram of measuring graphene sample's THz reflection by using THz-TDS system.

respectively. Raman spectroscopy is used to characterize the samples, which exhibited multilayer and nonuniform graphene distributions. Figure 4 shows the Raman spectrum of the basic graphene composite and graphene composite with DCMR array. The two obvious Raman spectrum peaks are G band at 1585 cm^{-1} and 2D band at 2686 cm^{-1}. The IG/I2D intensity ratio of multilayer graphene is larger than that of the monolayer graphene, and increases with layers of graphene [32]. As depicted in Figure 4d, the smallest IG/I2D intensity ratio of the graphene sample with SiO2 and silicon layers is 1.19, and the largest ratio is 1.76, which demonstrates that the sample owns multilayer graphene and the distribution of the graphene layers is nonuniform. For the graphene sample with integrated DCMR array, the maximum and minimum IG/I2D ratios are 1.21 and 1.17, as are shown in Figure 4b. The graphene layers of the sample without DCMR array are more than the one with DCMR array.

A THz time-domain spectroscopy (THz-TDS) system TAS7500 from Advantest Company is employed to measure the wideband THz absorption of the proposed designs by reflection configuration as is shown in Figure 5. The TAS7500 THz-TDS system covers the frequency from 0.2 to 2.0 THz with frequency resolution 7.6 GHz and peak power 50 mW. Highly doped silicon is chosen as the bottom layer of the graphene substrates to almost fully reflect THz wave on the interface between SiO_2 and silicon layer, and further isolate the absorption test influence of the thick silicon layer. The transmission coefficient of the two graphene samples, as is shown in Figure 1 of Appendix, is lower than −90 dB and is close to zero, which validates the full reflection of the highly doped silicon substrate.

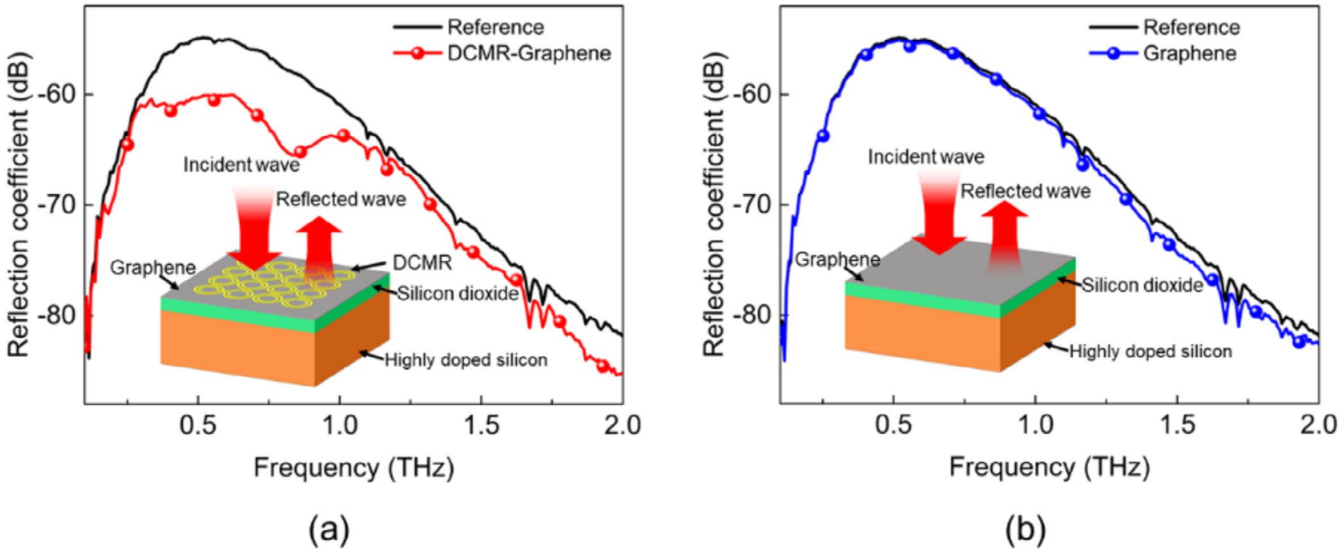

FIGURE 6 | Measured THz reflections of graphene samples with reference reflection: (a) graphene/SiO_2/Si with DCMR array; (b) graphene/SiO_2/Si.

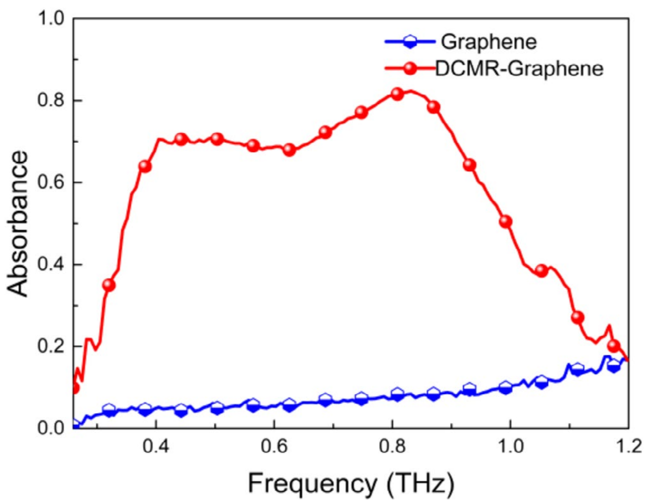

FIGURE 7 | Measured THz absorption of graphene samples with and without DCMR array.

First, measure the empty metal sample holder to obtain the total reflection signal Γref of the test system, and use it as a reference for calibrating the measurements of graphene samples. Reflection coefficients of two graphene samples with and without DCMR array are measured, respectively. The measured reflection coefficients of two graphene samples are shown in Figure 6 with reference reflection. The reflection of the basic graphene composite is very close to the reference reflection, which demonstrates very limited absorption of THz wave as shown in Figure 6b. However, the reflection of the graphene composite with DCMR array is lower in a broad frequency range from 0.3 THz to 1.1 THz, which shows obvious difference as shown in Figure 6a.

The THz absorption of graphene sample is calculated with formula $A_{gs} = \Gamma_{ref} - \Gamma_{gs}$, where A_{gs} and Γ_{gs} are the THz absorption and reflection of graphene samples, respectively. The THz absorbance of the graphene composite with DCMR array is much higher than that of the basic graphene composite in the full frequency range from 0.3 to 1.1 THz, as is shown in Figure 7. It proves that the DCMR array is able to enhance THz absorption ability of graphene effectively, with ultrawide fractional bandwidth of about 110% at its center frequency 0.7 THz. Over 70% THz absorption in the frequency range from 0.40 THz to 0.9 THz is achieved in the experiment. Moreover, the graphene composite with DCMR array absorbance achieves the highest value at around 0.85 THz. It is well consistent with the THz wave local enhancement of the DCMR array over frequency as is shown in the Figure 3, except for a frequency offset about 0.05 THz. The above experiments validate the simulated ultrawideband local confinement of THz wave on the DCMR array and ultrawideband high THz absorption enabled by DCMR array. For reference, Table 1 presents a comparison of the absorber performance between this work and other studies.

3 | Conclusion

In this work, we use the DCMR array to excite spoof surface plasmon polaritons (SPPs), which enhance both the graphene's THz absorption with an ultrawide bandwidth and the tolerance of graphene's physical impurities. The proposed DCMR array excites broadband spoof surface plasmon polaritons, increasing graphene's terahertz absorption to over 70% in the 0.40–0.90 THz range. The scheme is insensitive to graphene defects and layer nonuniformities, while the metal ring deposition process is simple and compatible with mass production.

A limitation lies in the passive nature of the current design, where the operating bandwidth and absorption rate are fixed by geometric parameters, lacking dynamic tunability. Future efforts will integrate electrically tunable graphene or phase-change materials for reconfigurable absorption, to advance practical applications in terahertz imaging, communication, and sensing.

TABLE 1 | Comparison of the present absorber with others.

	Graphene composite	Thickness	Bandwidth	Absorption	Bias voltage	Fabrication method	Fabrication complexity
[8]	Nonstructured graphene with dielectric resonators	95.2 μm	0.473–1.407 THz and 2.273–3.112 THz	> 10%	0ev	CVD growth	Medium
[13]	Graphene nanoribbon-ring cross structure	5.9 μm	3.5–3.75THz, ≈8.1THz and ≈10THz	> 25%, ≈78% and ≈90%	0.6ev	CVD graphene +EBL+etching	Medium
[15]	Periodically sinusoidally-patterned graphene layer	26.5 μm	1.0–2.0THz	> 13%	0ev	Electrostatic oping graphene sheet	Difficult
[32]	S-shaped graphene split-ring resonator	1.44 μm	7.2–7.5THz	> 70%	0.1ev	CVD graphene transfer+oxygen plasma etching	Medium
This work	Graphene patterned with DCMR array	500 μm	0.3–1.1 THz	> 70%	0ev	CVD+evaporator deposition technique	Medium

Author Contributions

H.E. Guo-Qiang, Johan Stiens, and Bart Kuyken conceived the experiments. H.E. Guo-Qiang, Cathleen De Tandt, Dries Van Thourhout, and Muhammad Muneeb fabricated the devices. Zhen-Yu Ding and Cheng Chen carried out the THz measurements and Raman measurements, respectively. H.E. Guo-Qiang and Zhen-Yu Ding did the simulation of THz transmission and reflection. All authors contributed to the manuscript.

Acknowledgments

This work is supported by the National Natural Science Foundation of China (NSFC) under Grant No. 62001280, Shanghai Pujiang Program (20PJ1404300), 111 Project (D20031), Guangxi Key Laboratory of Wireless Wideband Communication and Signal Processing, Guilin University of Electronic Technology (GXKL06200213), and the VUB through the SRP-project M3D2 and the ETRO-IOF project. This work also acknowledges the Advantest Company for offering the TDS test facilities.

Funding

This work is supported by the National Natural Science Foundation of China (NSFC) under Grant No. 62001280, Shanghai Pujiang Program (20PJ1404300), 111 Project (D20031), Guangxi Key Laboratory of Wireless Wideband Communication and Signal Processing, Guilin University of Electronic Technology (GXKL06200213), and the VUB through the SRP-project M3D2 and the ETRO-IOF project.

Conflicts of Interest

The authors declare no conflicts of interest.

Data Availability Statement

The data that support the findings of this study are available on request from the corresponding author. The data are not publicly available due to privacy or ethical restrictions.

References

1. Y. Hu, Z. Chen, Z. Yi, S. Cheng, S. Ahmad, and B. Li, “Ultra Wideband Solar Energy Absorption Device Based on Multi-Layered Ti-InAs Cylinder Metasurface,” *Physica E-Low-Dimensional Systems and Nanostructures* 180 (2026): 116514.

2. J. Luo, J. Guo, G. Zhao, et al., “Ultra-Wideband Solar Energy Absorption Device Based on Metal–Dielectric Symmetrical Gap Separation,” *Coatings* 16 (2026): 211.

3. H. Sheng, Y. Yi, Y. Guo, M. Liu, and Y. Yi, “Temperature-Switchable Double-Peak and Triple-Peak Narrow-Band Terahertz Absorbers Based on Vanadium Dioxide,” *Physica B: Condensed Matter* 728 (2026): 418399.

4. D. M. Mittleman, “Perspective: Terahertz Science and Technology,” *Journal of Applied Physics* 23 (2017): 230901.

5. M. Tonouchi, “Cutting-Edge Terahertz Technology,” *Nature Photonics* 1 (2007): 97–105.

6. A. Y. Nikitin, F. Guinea, F. J. Garcia-Vidal, and L. Martin-Moreno, “Surface Plasmon Enhanced Absorption and Suppressed Transmission in Periodic Arrays of Graphene Ribbons,” *Physical Review B: Condensed Matter* 8 (2012): 081405.

7. W. Gao, J. Shu, K. Reichel, et al., “High-Contrast Terahertz Wave Modulation by Gated Graphene Enhanced by Extraordinary Transmission Through Ring Apertures,” *Nano Letters* 3 (2014): 1242–1248.

8. L. Qi, C. Liu, and S. M. A. Shah, “A Broad Dual-Band Switchable Graphene-Based Terahertz Metamaterial Absorber,” *Carbon* 153 (2019): 179–188.

9. W. Ma, Z. Huang, X. Bai, P. Zhan, and Y. Liu, “Dual-Band Light Focusing Using Stacked Graphene Metasurfaces,” *ACS Photonics* 7 (2017): 1770–1775.

10. H. Chen, Z. Huang, Y. Huang, et al., “Consecutively Strong Absorption From Gigahertz to Terahertz Bands of a Monolithic Three-Dimensional Fe_3O_4/Graphene Material,” *ACS Applied Materials and Interfaces* 1 (2018): 1274–1282.

11. M. S. Islam, J. Sultana, M. Biabanifard, et al., “Tunable Localized Surface Plasmon Graphene Metasurface for Multiband Superabsorption and Terahertz Sensing,” *Carbon* 158 (2020): 559–567.

12. D. Xiao, M. Zhu, L. Sun, et al., "Flexible Ultra-Wideband Terahertz Absorber Based on Vertically Aligned Carbon Nanotubes," *ACS Applied Materials and Interfaces* 46 (2019): 43671–43680.

13. Z. Yi, J. Huang, C. Cen, et al., "Nanoribbon-Ring Cross Perfect Metamaterial Graphene Multi-Band Absorber in THz Range and the Sensing Application," *Results in Physics* 14 (2019): 102367.

14. S. Thongrattanasiri, F. H. Koppens, and F. J. G. De Abajo, "Complete Optical Absorption in Periodically Patterned Graphene," *Physical Review Letters* 4 (2012): 047401.

15. L. Ye, Y. Chen, G. Cai, et al., "Broadband Absorber With Periodically Sinusoidally-Patterned Graphene Layer in Terahertz Range," *Optics Express* 10 (2017): 11223–11232.

16. X. He, "Tunable Terahertz Graphene Metamaterials," *Carbon* 82 (2015): 229–237.

17. B. Sensale-Rodriguez, R. Yan, M. M. Kelly, et al., "Broadband Graphene Terahertz Modulators Enabled by Intraband Transitions," *Nature Communications* 1 (2012): 1–7.

18. A. Di Gaspare, E. A. A. Pogna, L. Salemi, et al., "Tunable, Grating-Gated, Graphene-on-Polyimide Terahertz Modulators," *Advanced Functional Materials* 31 (2021): 2008039.

19. H. Lin, B. C. Sturmberg, K. T. Lin, et al., "A 90-Nm-Thick Graphene Metamaterial for Strong and Extremely Broadband Absorption of Unpolarized Light," *Nature Photonics* 4 (2019): 270–276.

20. Z. Fang, S. Thongrattanasiri, A. Schlather, et al., "Gated Tunability and Hybridization of Localized Plasmons in Nanostructured Graphene," *ACS Nano* 7, no. 3 (2013): 2388–2395.

21. S. Ke, B. Wang, H. Huang, H. Long, K. Wang, and P. Lu, "Plasmonic Absorption Enhancement in Periodic Cross-Shaped Graphene Arrays," *Optics Express* 7 (2015): 8888–8900.

22. Y. Fan, N. H. Shen, T. Koschny, and C. M. Soukoulis, "Tunable Terahertz Meta-Surface With Graphene Cut-Wires," *ACS Photonics* 1 (2015): 151–156.

23. X. Cai, A. B. Sushkov, M. M. Jadidi, et al., "Plasmon-Enhanced Terahertz Photodetection in Graphene," *Nano Letters* 7 (2015): 4295–4302.

24. J. Zhang, Z. Zhu, W. Liu, X. Yuan, and S. Qin, "Towards Photodetection With High Efficiency and Tunable Spectral Selectivity: Graphene Plasmonics for Light Trapping and Absorption Engineering," *Nanoscale* 32 (2015): 13530–13536.

25. T. Low and P. Avouris, "Graphene Plasmonics for Terahertz to Mid-Infrared Applications," *ACS Nano* 2 (2014): 1086–1101.

26. Y. Li, K. Tantiwanichapan, A. K. Swan, and R. Paiella, "Graphene Plasmonic Devices for Terahertz Optoelectronics," *Nano* 7 (2020): 1901–1920.

27. E. Galiffi, J. B. Pendry, and P. A. Huidobro, "Broadband Tunable THz Absorption With Singular Graphene Metasurfaces," *ACS Nano* 2 (2018): 1006–1013.

28. Y. Sun, X. Qin, X. Yuan, Y. Huang, and H. Zhu, "Thermally Tunable Terahertz Metamaterial Absorber With Switchable Multi-Band Responses," *Physica Scripta* 100 (2025): 105544.

29. Z. Huang, H. Chen, Y. Huang, et al., "Ultra-Broadband Wide-Angle Terahertz Absorption Properties of 3D Graphene Foam," *Advanced Functional Materials* 2 (2018): 1704363.

30. G. He and J. Stiens, "Enhanced Terahertz Absorption of Graphene Composite Integrated With Double Circular Metal Ring Array," *Plasmonics* 5 (2018): 1705–1710.

31. Z. Tu, Z. Liu, Y. Li, et al., "Controllable Growth of 1–7 Layers of Graphene by Chemical Vapour Deposition," *Carbon* 73 (2014): 252–258.

32. O. H. Sinan, R. Barua, N. Dhar, and M. A. Rahman, "Graphene-Enabled Terahertz Metamaterial Absorber for Ultra-Wide Refractive Index Sensing," arXiv e-prints, arXiv (2025): 2511.01012.

Supporting Information

Additional supporting information can be found online in the Supporting Information section. **Figure S1:** Simulated transmission and reflection coefficients versus frequency for the inner radius of the small metal ranging from 10 to 100 μm: (a) transmission coefficient; (b) reflection coefficient. **Figure S2:** The simulated transmission and reflection coefficients versus frequency for the width of metal ring varying from 0.5 to 10 μm. (a) Transmission coefficient; (b) reflection coefficient. **Figure S3:** Measured THz transmission of graphene composite samples. DCMR-Graphene represents the graphene composite with DCMR array, and graphene represents the graphene composite sample without DCMR array. **Figure S4:** Schematic diagram of the transfer of graphene from the metal to the substrate. **Figure S5:** Schematic diagram of the DCMR array fabrication: (a) the mask is utilized to etch the DCMR array pattern; (b) the DCMR array is deposited on the graphene.